Missing-p_T-plus-jets signal for heavy leptons in $p\bar{p}$ collisions

V. Barger and J. Ohnemus
Physics Department, University of Wisconsin, Madison, Wisconsin 53706

R. J. N. Phillips
Rutherford Appleton Laboratory, Chilton, Didcot, Oxon, England
(Received 1 May 1986)

The most promising signal for the production of fourth-generation heavy leptons at $p\bar{p}$ colliders in the weak subprocess $d\bar{u}\to W\to L\bar{\nu}_L$ with $L\to\nu_L q\bar{q}'$ decay would be the appearance of events with large missing p_T plus jets. This signal is reexamined, taking into account additional QCD gluon jets from $d\bar{u}\to Wg$ production, using the full seven-particle matrix element square obtained by helicity-projection techniques. It is compared to standard physics backgrounds arising from $W\to\tau\bar{\nu}$, $Z\to\nu\bar{\nu}$, and heavy-quark decay processes at CERN and Fermilab energies; the backgrounds are comparable to the L signal but can in principle be separated from it in various ways.

I. INTRODUCTION

A possible heavy charged lepton L, belonging to a fourth generation of standard-model fermions, would be produced in $p\bar{p}$ collisions via W production with $W\to L\bar{\nu}_L$ decay, provided that $m_L+m_{\nu_L}<M_W$. The most easily distinguished signal for L would then be the decay $L\to\nu_L q\bar{q}'$ leading typically to events with large missing p_T and two jets[1] (the leptonic decay signature[1,2] is much harder to discriminate from background). However, the jet structure of W-decay events is affected by additional gluons radiated from the incident quarks. In the present paper we present a reexamination of the events with two jets plus missing p_T (denoted $\not{p}_T$ henceforth) arising from $W\to L\bar{\nu}_L$, taking into account the dominant correction coming from $d\bar{u}\to Wg$ production and using the complete seven-particle $d\bar{u}\to\nu_L q\bar{q}'g$ matrix element derived by helicity-projection techniques.[3]

Our calculations are based on the truncated shower approximation[4,5] where the complete QCD shower of partons emitted during W production is approximated by the dominant lowest-order QCD subprocess $q\bar{q}'\to Wg$, as described in Sec. II. Complete spin correlation through the seven-particle production and decay chain

$$d\bar{u}\to Wg\to L\bar{\nu}_L g\to\nu_L\bar{\nu}_L q\bar{q}'g \tag{1}$$

(see Fig. 1) is included in the squared matrix element as described in Sec. III. The pair of neutrinos (assumed to be light) lead typically to events with large $\not{p}_T$; the three final partons $q\bar{q}'g$ are interpreted in terms of 0, 1, 2, or 3 jets following the UA1 jet algorithm. Distributions of physical interest, for events of $W\to L\bar{\nu}_L$ origin, with large $\not{p}_T$ and two jets have been calculated at $\sqrt{s}=630$ and 2000 GeV, corresponding to the CERN and Fermilab $p\bar{p}$ collider energies. These are presented in Sec. IV for $m_L=25$, 40, and 60 GeV and compared to the principal standard-model backgrounds from $W\to\tau\bar{\nu}$, from Z+jets production with $Z\to\nu\bar{\nu}$ decay, and from heavy-quark production with semileptonic decays. Section V contains discussion; we conclude that the backgrounds are comparable to the predicted L signals, but can in principle be separated in various ways.

It is possible that the neutrinos ν_L and $\bar{\nu}_L$ in Eq. (1) are also heavy and decay by charged-current couplings. This scenario has been studied in Ref. 6, in the context of exotic E_6 leptons. It gives quite different signals.

It should, of course, be remembered that heavy leptons can also be sought at e^+e^- colliders, where the $L\bar{L}$ signal would be large. Present experiments place the limit $m_L>23$ GeV. Near future experiments at the Z^0 resonance will allow the range $m_L\lesssim\frac{1}{2}M_Z$ to be studied.

II. TRUNCATED SHOWER APPROXIMATION

The total cross section for $W^\pm$ production in $p\bar{p}$ collisions is calculable from the primary process $q\bar{q}'\to W$ convoluted over quark distributions that have been evolved up to the scale $Q^2=M_W{}^2$, multiplied by the factor $K=1+(16\pi^2/9)[\alpha_s(M_W{}^2)/2\pi]$ for higher-order corrections not already included in the evolution. This Q^2 evolution of quark distributions, however, implies the presence of radiated quarks and gluons accompanying the interacting $q\bar{q}'$ pair, plus a nontrivial distribution of $p_T(W)$. To make this QCD radiation and $p_T(W)$ dependence explicit calls for a Monte Carlo shower calculation;[7–12] however, the principal physical features of such a shower are economically reproduced at the energies of present interest by the dominant lowest-order QCD subprocess $q\bar{q}'\to Wg$ alone. This subprocess cross section (multiplied by K) gives the correct behavior at large

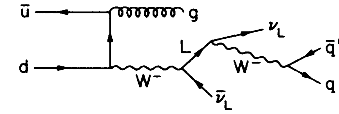

FIG. 1. The production and decay chain $d\bar{u}\to Wg$, $W\to L\bar{\nu}_L$, $L\to\nu_L q\bar{q}'$.

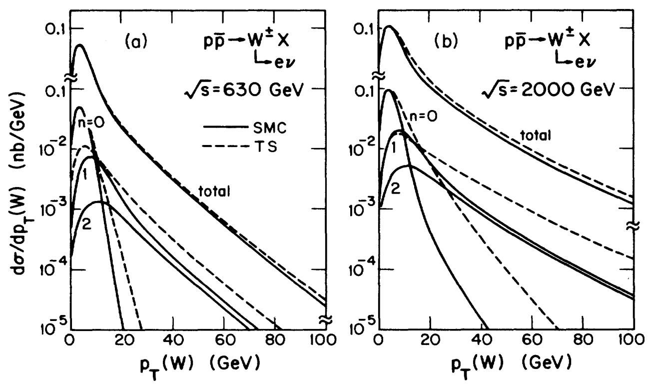

FIG. 2. The dependence of inclusive $p\bar{p}\to W+X\to e\nu+X$ production on $p_T(W)$: a comparison of the truncated shower (TS) approximation with the complete shower Monte Carlo (SMC) of Ref. 12. Predictions of $d\sigma/dp_T(W)$ are plotted versus $p_T(W)$ at $\sqrt{s}=630$ and 2000 GeV; the contributions from zero, one, and two-jet events are also shown separately. Solid curves denote SMC, dashed curves denote TS.

$p_T(W)$; it gives the correct total cross section if the ${p_T}^{-2}$ divergence is cut off by an empirical factor

$$f({p_T}^2)=1-\exp[-{p_T}^2/(p_{T\,\mathrm{cut}})^2]\ , \tag{2}$$

where $p_{T\,\mathrm{cut}}=2.0$ and 3.45 GeV for $\sqrt{s}=630$ and 2000 GeV, respectively, and finally it reproduces the dominant zero-jet plus one-jet character of the full shower calculation.[12] This truncated shower approximation[4,5] plainly does not give the fine details of small-p_T dependence, but these details are arguably smeared over by experimental resolution in practical calculations, so that nothing important has been lost.

Figure 2 compares the cross-section dependence on $p_T(W)$ predicted by the truncated shower approximation with that of the complete shower Monte Carlo of Ref. 12, for inclusive $W\to e\nu$ production and separately zero-jet and one-jet events [requiring $p_T(\mathrm{jet})\geq 5$ GeV]. This figure shows reasonable agreement with the dominant features throughout. Where there are large discrepancies, in zero-jet events at large p_T or one-jet events at very small and very large p_T, the components in question are only a small part of the cross section. Table I compares the jet fractions from the full and the approximate shower calculations.

We use this same approach for our present study of $W\to L\bar{\nu}_L$ decay signatures. We approximate the QCD showers accompanying W production by single-gluon radiation and base our calculation entirely on the production and decay chain of Eq. (1). The matrix element for this seven-particle amplitude is written down in Sec. III. We apply the empirical cutoff of Eq. (2) and the K factor to secure the correct total cross section.

Since we shall consider only events with large missing p_T [which almost always have one or two additional decay jets from q and $\bar{q}$ in Eq. (1)], the truncated shower approximation is adequate for discussing $n\leq 2$ jets and also describes the case $n=3$ to the extent that two jets come from L decay. We have confirmed by test calculations with a full shower Monte Carlo that our results are essentially correct in this sector; fortunately it contains a large fraction of L events.

III. COMPLETE AMPLITUDES

The squared matrix element for the seven-particle amplitude of Eq. (1) can be evaluated directly by γ-matrix reduction routines, but this leads to enormously complicated algebraic expressions that are very hard to simplify. However, great simplification results if we factor the amplitude into L-production and L-decay parts (that are separately much simpler than the complete production/decay chain). This is the helicity-projection approach.[3]

The situation is particularly simple when both the production and decay couplings of L are pure $V-A$, which is the case of present interest. Then the spin color-averaged squared matrix elements for *any* such production and decay depend linearly on the L momentum and can be expressed as

$$\begin{aligned}|\mathcal{M}(L\ \text{production})|^2&={N_i}^{-1}(X\cdot L)\ ,\\ |\mathcal{M}(L\ \text{decay})|^2&=(Y\cdot L)\ ,\end{aligned} \tag{3}$$

where X and Y are four-vectors relating to the production and decay kinematics, respectively. N_i is the number of initial spin/color states and L is the heavy-lepton momentum. In deriving these expressions, it is essential to keep track throughout of the momentum vector L in the heavy-lepton tensor. It has been shown[3] that a general prescription for the spin/color-average squared matrix element of the complete production/decay chain is then

$$|\mathcal{M}|^2={N_i}^{-1}[(X\cdot L)(Y\cdot L)-\tfrac{1}{2}{m_L}^2(X\cdot Y)]/|D|^2\ , \tag{4}$$

where $D=(L^2-{m_L}^2+im_L\Gamma_L)$ is a propagator denominator.

For the case of Eq. (1), the relevant L production[13] and decay matrix elements are known and give

TABLE I. Comparison of the shower Monte Carlo (SMC) and the truncated shower (TS) predictions for the fraction of $p\bar{p}\to W$ events with jet multiplicity $n=0,1,2,3$ at $\sqrt{s}=630$ and 2000 GeV.

$\sqrt{s}$	630 GeV				2000 GeV			
n	0	1	2	3	0	1	2	3
SMC	0.69	0.23	0.07	0.01	0.55	0.28	0.12	0.03
TS	0.66	0.34			0.71	0.29		

$$X_\alpha = \frac{4\pi\alpha_s G_F{}^2 M_W{}^4 |U_{ud}|^2}{[(x^2-M_W{}^2)^2+M_W{}^2\Gamma_W{}^2]} 512(g\cdot d)^{-1}(g\cdot\bar{u})^{-1}\{(\bar{\nu}\cdot d)(g\cdot\bar{u})d_\alpha - (\bar{\nu}\cdot d)(x\cdot d)g_\alpha + [(\bar{\nu}\cdot d)(x\cdot\bar{u}) - (\bar{\nu}\cdot g)(x\cdot\bar{u}) + (\bar{\nu}\cdot d)(x\cdot d) + (\bar{\nu}\cdot\bar{u})(g\cdot d)]\bar{u}_\alpha\}\ , \tag{5}$$

$$Y_\alpha = \{384 G_F{}^2 M_W{}^4 |U_{qq'}|^2 (q\cdot\nu)/[(y^2-M_W{}^2)^2+M_W{}^2\Gamma_W{}^2]\}\bar{q}'_\alpha\ , \tag{6}$$

and $N_i=36$; hence, we infer the spin/color-averaged matrix element squared for the complete process:

$$|\mathcal{M}|^2 = F(g\cdot d)^{-1}(g\cdot u)^{-1}|D'|^{-2}(q\cdot\nu)\{[2(L\cdot d)(L\cdot\bar{q}') - m_L{}^2(d\cdot\bar{q}')](\bar{\nu}\cdot d)(g\cdot\bar{u}) - [2(L\cdot g)(L\cdot\bar{q}') - m_L{}^2(g\cdot\bar{q}')](\bar{\nu}\cdot d)(x\cdot d) + [2(L\cdot\bar{u})(L\cdot\bar{q}') - m_L{}^2(\bar{u}\cdot\bar{q}')][(\bar{\nu}\cdot d)(x\cdot\bar{u}) - (\bar{\nu}\cdot g)(x\cdot\bar{u}) + (\bar{\nu}\cdot d)(x\cdot d) + (\bar{\nu}\cdot\bar{u})(g\cdot d)]\}\ . \tag{7}$$

Here D' is a product of W and L propagator denominators

$$D' = (L^2 - m_L{}^2 + i m_L\Gamma_L)(x^2 - M_W{}^2 + iM_W\Gamma_W)(y^2 - M_W{}^2 + iM_W\Gamma_W)\ , \tag{8}$$

with $x=d+\bar{u}-g$ and $y=q+\bar{q}'$. F contains the remaining numerical factors

$$F = \left[\frac{2^{15}}{3}\right]\pi\alpha_s G_F{}^4 M_W{}^8 |U_{ud}|^2 |U_{qq'}|^2\ , \tag{9}$$

where U_{ij} is the Kobayashi-Maskawa quark mixing matrix. We consistently use particle labels to denote their four-momenta and abbreviate $\nu_L, \bar{\nu}_L$ to $\nu, \bar{\nu}$ in the preceding formulas. We use standard conventions, such that the cross-section formula is

$$d\sigma(d\bar{u}\to\nu\bar{\nu}q\bar{q}'g) = \frac{1}{2\hat{s}}|\mathcal{M}|^2\left[\prod_{k=\nu,\bar{\nu},q,\bar{q}',g}\frac{d^3k}{2E_k}\right](2\pi)^{-11}\delta^4(d+\bar{u}-\nu-\bar{\nu}-q-\bar{q}'-g) \tag{10}$$

summed (averaged) over final (initial) spins and colors.

IV. CALCULATIONS

We have calculated the production cross section and distributions for the subprocess Eq. (1) and its CP conjugate, folded with the quark distribution of Glück, Hoffmann, and Reya,[14] evolved up to $Q^2=\hat{s}$ using $\Lambda=0.4$ GeV. The choice of quark distribution model is not critical for W production, since presently available models[14,15] give very similar results and the latter can in any case be normalized to the $W\to l\bar{\nu}$ data. However, Z production at large p_T and hence the $Z\to\nu\bar{\nu}$ background[16] differ appreciably between models and the $Z\to l\bar{l}$ data are not yet precise enough to decide the choice. We use the model of Ref. 14 here because it gives the largest $Z\to\nu\bar{\nu}$ background (see Fig. 3).

The final partons q, $\bar{q}'$, and g were regarded as potential jets; they were coalesced if their angular separations satisfied $(\Delta\eta)^2+(\Delta\phi)^2\le 1$ where $\eta=\ln\cot(\frac{1}{2}\theta)$ is the pseudorapidity and θ and ϕ are polar and azimuthal angles with respect to the $p\bar{p}$ beam axis. Finally they were identified as experimentally observable hadron jets if they had $p_T\ge 5$ GeV and $|\eta|<2.5$.

It is known from the absence of a signal in e^+e^- collider experiments[17] that $m_L>22.7$ GeV while for $m_L\gtrsim M_W$ the present production mechanism is kinematically suppressed. We therefore illustrate the range of interest by the examples $m_L=25$, 40, and 60 GeV.

We compare the heavy-lepton signals with the following principal standard-model backgrounds at large $\not{p}_T$.

(i) Contributions from the case $L=\tau$ (where the q and $\bar{q}'$ contributions always coalesce).

(ii) Contributions from $p\bar{p}\to Z+$jets with $Z\to\nu\bar{\nu}$ de-

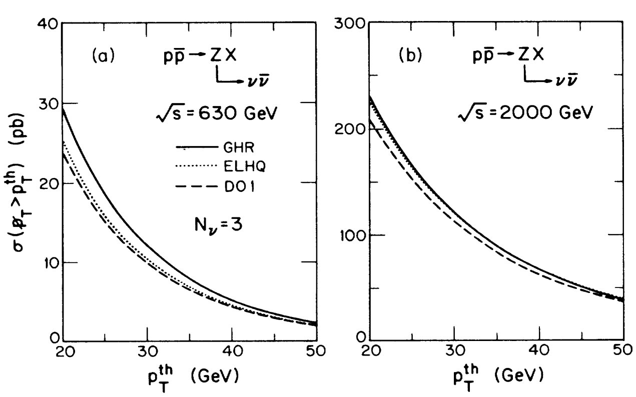

FIG. 3. Dependence of the $Z\to\nu\bar{\nu}$ background on choice of parton distributions; the calculated cross section for $p\bar{p}\to Z+X\to\nu\bar{\nu}+X$ with $\not{p}_T$ greater than a threshold $p_T^{\rm th}$ is plotted versus $p_T^{\rm th}$ at $\sqrt{s}=630$ and 2000 GeV. The solid, dotted, and dashed curves are based on the models of Glück, Hoffmann, and Reya,[14] Eichten *et al.*,[15] and Duke-Owens set one,[15] respectively. Three generations of neutrinos are assumed.

cay, calculating the former from the QCD-shower model of Ref. 12 and assuming from three to six generations of light neutrinos.

(iii) Production of $b\bar{b}$ and $c\bar{c}$ heavy-quark pairs, with semileptonic decays (including the $b \to c \to s$ cascade and the possibility of multiple neutrinos); here we used a truncated shower approximation to include the production of an additional light quark or gluon, with no K-factor enhancement since none is needed to describe dimuon data.[5] The details of this calculation are given in Ref. 5. The calculation is based upon $q\bar{q} \to Q\bar{Q}g$, $gq \to Q\bar{Q}q$, and $gg \to Q\bar{Q}g$ subprocesses ($Q = b,c$) with a cutoff in the variable $p_T(Q\bar{Q})$ to remove soft and collinear divergences, adjusted to give the correct cross section and dependence on $m(Q\bar{Q})$. This cutoff takes effect around $p_T = 2$ to 3 GeV like that of Eq. (2); here the recoiling light parton is in a region where it contributes very little to jets. We make the approximation $m_Q = 0$ in the matrix elements at large p_T: the cutoff is rather insensitive to this procedure.

(iv) Hadroproduction of $t\bar{t}$ pairs and weak $W \to t\bar{b}$ production with semileptonic decays of heavy quarks (including the full $t \to b \to c \to s$ cascade). We use $O(\alpha_s^2)$ QCD for the former (a massless $Q\bar{Q}$ treatment is not applicable here), ignoring the small contributions to jets from additional gluons compared to the large contributions from t and $\bar{t}$ decays. We use a truncated shower approximation for W production with $W \to t\bar{b}$ decay.

In both (iii) and (iv), events with charged leptons of $p_T > 3.5$ GeV are excluded. A top-quark mass of 40 GeV is generally assumed.

Figures 4(a)—4(d) show first the cross sections for $\not{p}_T$ greater than a given threshold $p_T{}^{\text{th}}$, versus p_T^{th}, summed over $n = 0,1,2,3$ jets at $\sqrt{s} = 630$ GeV and 2 TeV. To avoid confusion, the comparisons with backgrounds (i) + (ii) and (iii) + (iv) are made separately. These figures show clearly that the heavy-lepton signal is swamped by background if the threshold is set too high. It is also true that the $b\bar{b} + c\bar{c}$ background overwhelms the L signal at small $\not{p}_T$ (seen explicitly in the 2-TeV comparison). As a compromise we shall henceforth choose the threshold to be $\not{p}_T \geq 20$ GeV. It also shows that the principal background with this $\not{p}_T$ threshold comes from τ events. Figure 5 gives the decomposition of the L, τ, and Z cross sections into one- and two-jet events.

Table II gives the cross sections for L and background events that have $n = 0,1,2,3$ jets. The jet multiplicity n depends on the jet threshold; two cases $p_T(\text{jet}) \geq 5$ GeV and $p_T(\text{jet}) \geq 10$ GeV are given. The table shows that τ and Z backgrounds are distributed toward lower n values

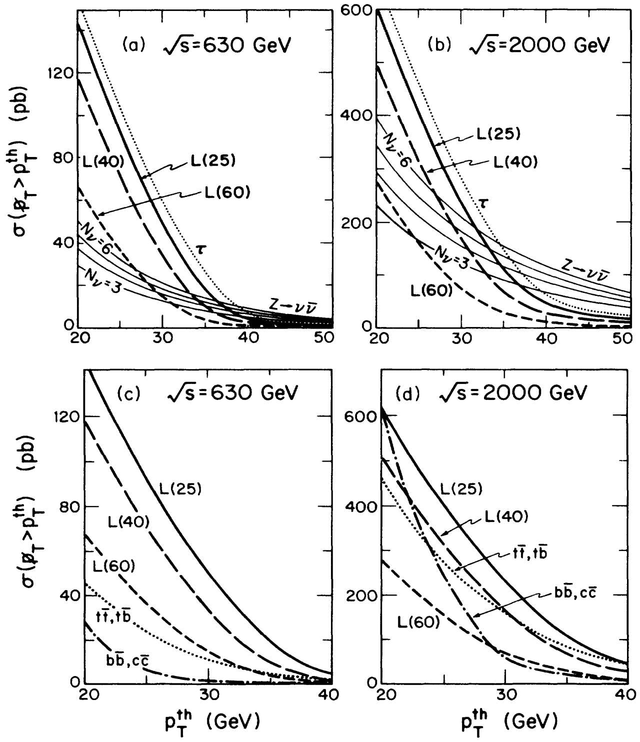

FIG. 4. Calculated cross sections for $\not{p}_T$ greater than a threshold p_T^{th}. σ ($\not{p}_T > P_T^{\text{th}}$) is plotted versus p_T^{th}. Solid, long-dashed, and short-dashed curves denote the $W \to L\nu$ signal, for $m_L = 25$, 40, and 60 GeV, respectively. (a) A comparison with the $W \to \tau\nu$ (dotted curve) and $Z \to \nu\bar{\nu}$ for $f = 3,4,5,6$ generations of light neutrinos (thin solid curves), at $\sqrt{s} = 630$ GeV; (b) as (a), but at $\sqrt{s} = 2$ TeV; (c) a comparison with $b\bar{b} + c\bar{c}$ (dot-dashed curve) and $t\bar{t} + t\bar{b}$ (dotted curve) backgrounds at $\sqrt{s} = 630$ GeV; (d) as (c), but at $\sqrt{s} = 2$ TeV.

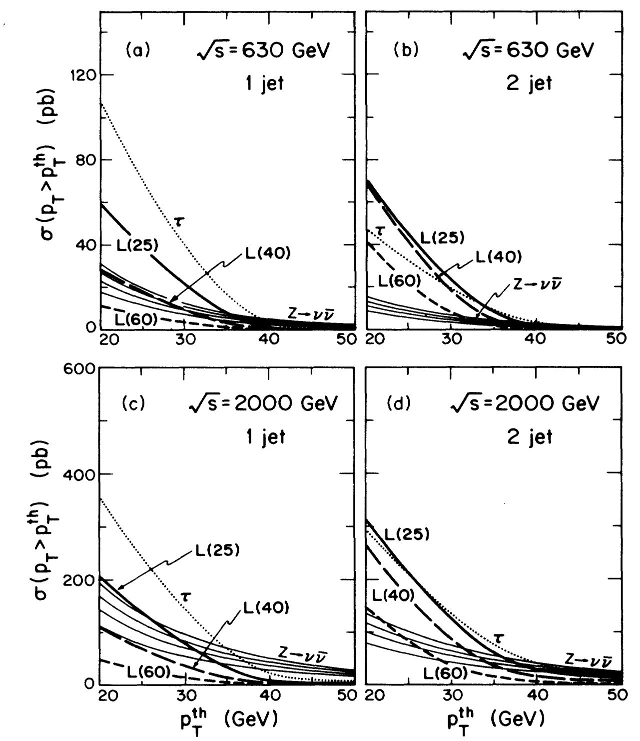

FIG. 5. One- and two-jet cross sections for $\not{p}_T$ greater than a threshold p_T^{th}. (a) and (b) show the decomposition of Fig. 4(a) into one- and two-jet components, respectively; (c) and (d) show the decomposition of Fig. 4(b) into one- and two-jet components, respectively.

TABLE II. Cross sections in pb for L and background events with jet multiplicity $n=0,1,2,3$ at $\sqrt{s}=630$ and 2000 GeV.

Threshold		$p_T(\text{jet})\geq 5$ GeV				$p_T(\text{jet})\geq 10$ GeV		
n	0	1	2	3	0	1	2	3
			$\sqrt{s}=630$ GeV					
$L(25)$		58	70	14	0.2	105	35	2
$L(40)$		27	68	20	0.2	65	46	4
$L(60)$		11	41	13	0.4	26	35	4
τ		106	47	0		133	20	0
Z		17	9	2	0.1	23	5	0.3
$t\bar{t},t\bar{b}$		2	19	16	0.1	11	21	10
$b\bar{b},c\bar{c}$			22	11		8	21	4
			$\sqrt{s}=2000$ GeV					
$L(25)$	7	200	305	80	14	373	192	13
$L(40)$	4	106	255	115	10	243	197	30
$L(60)$	2	47	141	76	3	103	137	23
τ	11	349	287	0	18	471	158	0
Z	7	111	79	24	11	151	51	8
$t\bar{t},t\bar{b}$	1	36	141	174	5	100	190	127
$b\bar{b},c\bar{c}$	0.2	11	480	220	1	65	545	100

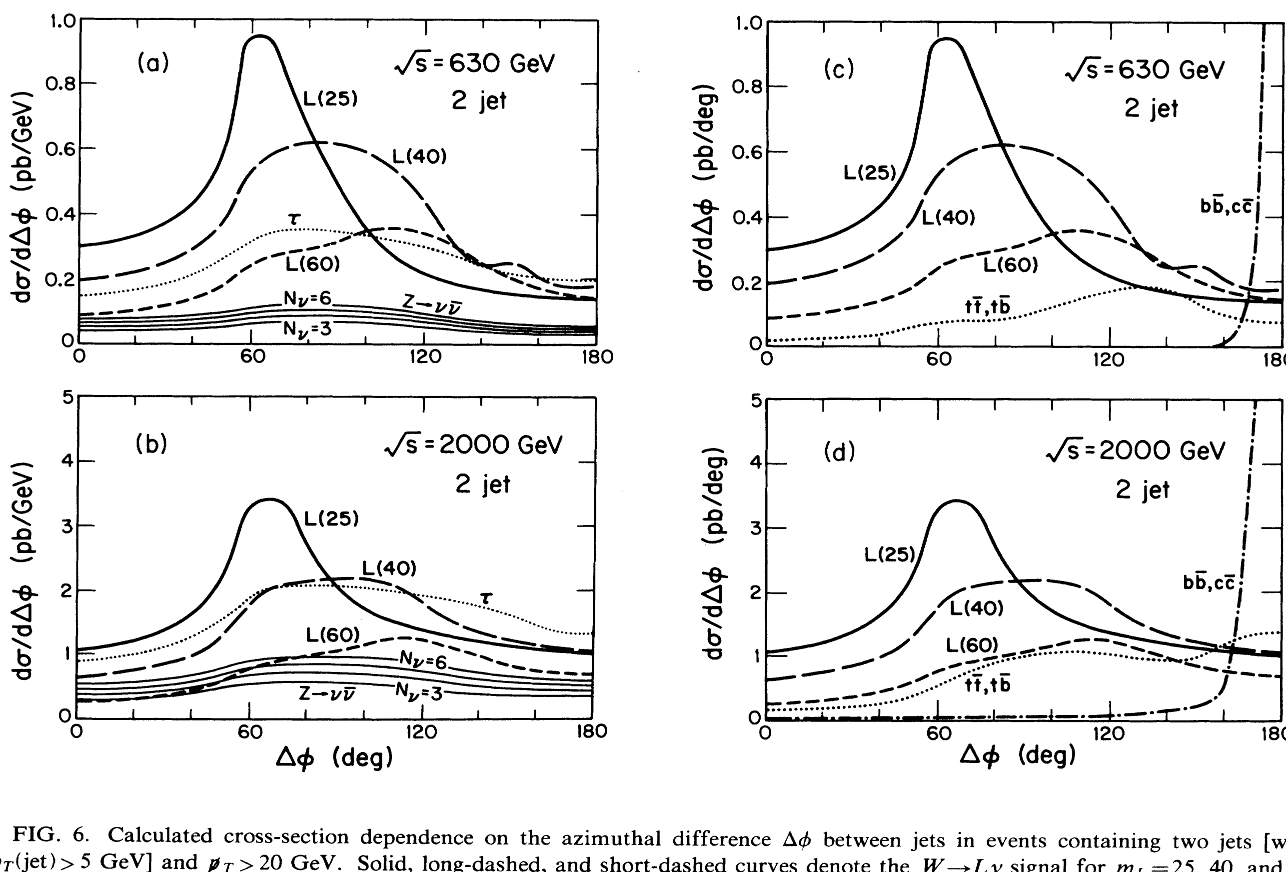

FIG. 6. Calculated cross-section dependence on the azimuthal difference $\Delta\phi$ between jets in events containing two jets [with $p_T(\text{jet})>5$ GeV] and $\not{p}_T>20$ GeV. Solid, long-dashed, and short-dashed curves denote the $W\to L\nu$ signal for $m_L=25$, 40, and 60 GeV, respectively. (a) A comparison with $W\to\tau\nu$ (dotted curve) and $Z\to\nu\bar{\nu}$ (thin solid curves) for $f=3,4,5,6$ generations of light neutrinos, at $\sqrt{s}=630$ GeV; (b) as (a), but at $\sqrt{s}=2$ TeV; (c) a comparsion with $b\bar{b}+c\bar{c}$ (dot-dashed curve) and $t\bar{t}+t\bar{b}$ (dotted curve) backgrounds at $\sqrt{s}=630$ GeV; (d) as (c), but at $\sqrt{s}=2$ TeV.

than the L signal, whereas the heavy-quark backgrounds have a higher mean jet multiplicity. There is some advantage in selecting two-jet events, since they contain more measurable parameters than one-jet events. For $n=2$, the overall signal-to-background rate does not depend critically on the choice of jet threshold, but the absolute value of the signal is generally bigger for the 5-GeV threshold. Henceforth we shall concentrate attention on events with $n=2$ jets with $p_T(\text{jet}) \geq 5$ GeV and $|\eta(\text{jet})| < 2.5$.

Figures 6(a)–6(d) show the distribution in azimuthal difference $\Delta\phi$ between the jets in $\not{p}_T$ + two-jet events for L and background events. In all cases, there is a dip in the region of $\Delta\phi = 0$ which is simply attributable to jet coalescence [two jets are combined when $(\Delta\eta)^2 + (\Delta\phi)^2 \leq 1$ so the region $\Delta\phi \leq 1$ suffers some suppression]. The $L(25)$ signal, which would peak at $\Delta\phi = 0$ but for the coalescence condition, has a peak near $\Delta\phi = 1$ rad $= 57°$. The $L(40)$ and $L(60)$ signals have broader maxima which can be understood as due to the greater energy release in these cases. Apart from dips at small $\Delta\phi$, the τ, Z, and $t\bar{t} + t\bar{b}$ backgrounds are all broadly isotropic but the $b\bar{b} + c\bar{c}$ background is very sharply peaked near $\Delta\phi = 180°$.

An important additional feature of the L signal is that in approximately $\frac{1}{2}$ of the events one jet will contain a charge quark, coming from $L \to \nu_L \bar{c} s(d)$. The resulting charm particle can in principle be recognized directly from its decay by a microvertex detector. Figure 7 shows the predicted distributions of this charm particle (assuming the fragmentation model of Ref. 18) with respect to laboratory energy, p_T, and azimuthal angle relative to $\not{p}_T$. These distributions could provide additional checks on an eventual L signal.

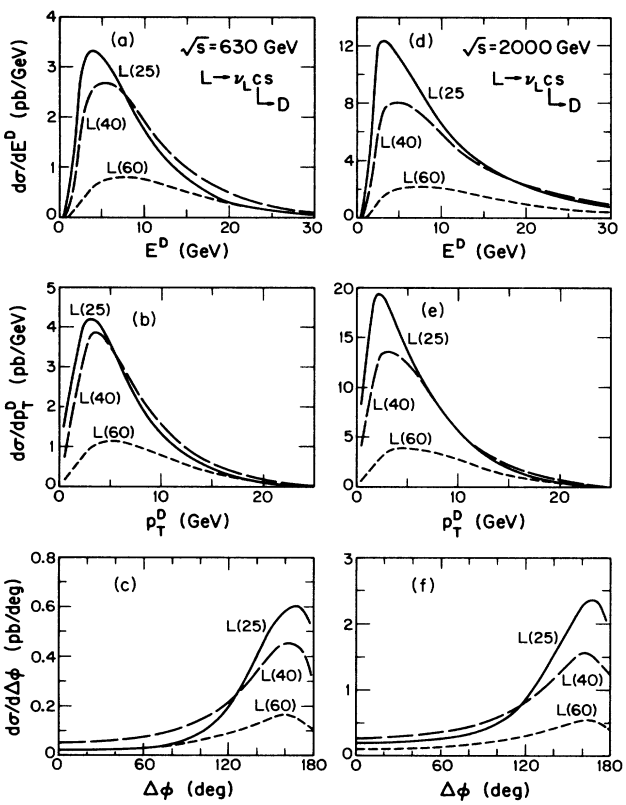

FIG. 7. Predicted distributions of the charm particle arising from $L \to \nu_L s\bar{c}$ decays in events with two jets of $p_T > 5$ GeV plus $\not{p}_T > 20$ GeV. Distributions are shown versus (a) laboratory energy at $\sqrt{s} = 630$ GeV; (b) p_T at $\sqrt{s} = 630$ GeV; (c) azimuthal angle ϕ relative to $\not{p}_T$ at $\sqrt{s} = 630$ GeV; (d),(e),(f) are as (a),(b),(c), respectively, but at $\sqrt{s} = 2$ TeV.

Finally, note that the $t\bar{t}$ and $t\bar{b}$ backgrounds illustrated above are for $m_t = 40$ GeV; they contribute in the ratio 1:1 at $\sqrt{s} = 630$ GeV, 2:1 at $\sqrt{2} = 2$ TeV. If t were lighter, the $t\bar{t}$ part would increase but $t\bar{b}$ would change little. If t were as light as 25 GeV (which seems unlikely[19]), the overall t background would increase by about 2.5 at $\sqrt{s} = 630$ GeV and by about 3.5 at $\sqrt{s} = 2$ TeV, for $\not{p}_T > 20$ GeV and $n = 2$.

V. DISCUSSION

The present integrated luminosity at the CERN $p\bar{p}$ collider is already about 0.7 pb^{-1} per intersection and more is planned. The future luminosities at Fermilab will be greater. Table II shows that an L signal in two-jet events with $\not{p}_T > 20$ GeV could already have produced some dozens of events at CERN (assuming a detection efficiency of order 50%); at Fermilab, some hundreds of such events might be anticipated. Such signals could be significant. The question is whether standard physics backgrounds can be separated.

The $W \to \tau\nu$ background, though larger than the L signal, should not pose serious problems. The number and distribution of events can be accurately calculated from experimental observations of $W \to e\nu, \mu\nu$ events. Also the $\tau \to \nu q\bar{q}'$ hadronic jets have quite distinctive low invariant mass and low multiplicity, so that many of these events can be identified directly.[20] Finally, the τ-decay vertex can in principle be resolved by a microvertex detector; the topological difference between this case and a charm decay from $L \to \nu s\bar{c}$ would be that the τ-decay products have no accompanying hadrons from fragmentation.

The $Z \to \nu\bar{\nu}$ background calculations can in principle be related to $Z \to e^+e^-, \mu^+\mu^-$ events, but the latter are still not accurately normalized. More importantly, the number of light neutrino species is unknown. The signal could be separated by $\Delta\phi$ dependence for $m_L = 25$ GeV but not for $m_L = 40$–60 GeV. However, the fact that neither of the two accompanying jets is usually generated by a charm quark can in principle clearly separate this background from L signals.

The $b\bar{b}$ and $c\bar{c}$ backgrounds are at first sight a very serious problem, especially at the Fermilab energy. Fortunately the $\Delta\phi$ dependence is dramatically peaked near 180°. A cut in $\Delta\phi$ can essentially remove this background completely.

Finally, there is a background from $t\bar{t}$ and $W \to t\bar{b}$ sources. With the mass assumption $m_t = 40$ GeV illustrated in Table II and Figs. 4–6, it is not a serious problem at $\sqrt{s} = 630$ GeV; consider, for example, Fig. 6(c) with a cut $\Delta\phi \leq 100°$. However, it looms larger at $\sqrt{s} = 2$ TeV (and at either energy if m_t is lower). The most distinctive feature of this class of contributions is the large number of short but resolvable decay vertices. Remembering that the normal decay route is $t \to b \to c \to s$, we see that $t\bar{t}$ events contain at least four b- and c-decay vertices while $W \to t\bar{b}$ events contain at least three. Furthermore,[21] a large fraction of events (70% for $t\bar{t}$, 45% for $t\bar{b}$) contain additional c- or τ-decay vertices arising from the multibranch modes $t \to bc\bar{s}, b\nu\bar{\tau}$ or $b \to cs\bar{c}, c\tau\bar{\nu}$. This high vertex multiplicity distinguishes these background events from the L signal, if a microvertex detector is available.

To summarize the discussion thus far, it appears that all standard physics backgrounds can be distinguished or separated in principle, but in many cases a microvertex detector is either required or desirable. Until recently no such detector has been running at CERN. Let us now consider the prospects for immediate or future detection of L for different mass regions.

(i) $m_L = 25$—40 GeV. In this case the expected signal at CERN is much larger than the $t\bar{t} + t\bar{b}$ backgrounds (we assume $m_t = 40$ GeV, make a cut $\Delta\phi < 170°$ to remove $b\bar{b} + c\bar{c}$ backgrounds and assume that most of the $W \to \tau\nu$ events are identified or calculated and removed). The L signal for present luminosity ($\simeq 1$ pb^{-1}) could already be of order 35 events, on top of a $Z + t\bar{t} + t\bar{b}$ background of order 15 events plus some events from uncertainties in removing $W \to \tau\nu$. Statistically such numbers would be quite significant, but they rely on theoretical estimates of the background rates and on the t mass. With this caveat, detection at CERN would seem quite practicable now or soon, even without a vertex detector. At Fermilab energy the signal-to-background ratio would be smaller but the statistics from a luminosity of 1 pb^{-1} would be much better. With a microvertex detector, quite a clean experiment would be possible. In this mass range, m_L could be determined from the $\Delta\phi$ dependence of the signal.

(ii) $m_L \simeq 60$ GeV. In this case the signal would be much smaller, say 20 events instead of 35 for the present CERN luminosity. The statistics would now be more marginal. Also the $\Delta\phi$ dependence would be much more like the background, leaving nothing but the rate to distinguish it (in the absence of microvertex detection). However, with a microvertex detector, the measurement of a signal from L in this mass range looks quite feasible for the future; m_L would have to be determined from the rate.

(iii) $m_L > 60$ GeV. As m_L approaches M_W, the qualitative distributions of final particles change little, but the overall $W \to L\nu_L$ rate is progressively suppressed by the factor

$$f = (1-x)(1 - \tfrac{1}{2}x - \tfrac{1}{2}x^2) , \qquad (11)$$

where $x = (m_L / M_W)^2$. This is only slightly offset by a higher probability of L events producing $\not{p}_T > 20$ GeV. For $m_L = 70$ GeV, the signal is suppressed by about 2.5 relative to the $m_L = 60$ GeV case. Eventually the signal will be lost behind the residual uncertainties remaining after removal of backgrounds. Experimental sensitivity could ultimately extend some way beyond $m_L = 60$ GeV.

If no such signals are detected, it will be possible to exclude a sequential heavy lepton L in the corresponding mass ranges (below M_W). If a signal *is* found, distinct from the standard physics backgrounds, the question will be whether it comes from L or some other new physics. Identity checks for L will include the various dynamical distributions, the $\sqrt{s}$ dependence and the fact that half the $L \to \nu q\bar{q}'$ events should contain a charm jet. To summarize, if L exists then (i) appreciable L signals are expected at $p\bar{p}$ colliders, in two-jet events with $\not{p}_T > 20$ GeV, up to $m_L = 60$ GeV and perhaps beyond, (ii) standard physics backgrounds from $W \to \tau\nu$, $Z \to \nu\bar{\nu}$, and heavy quarks can all in principle be identified or excluded, and (iii) microvertex detection could play a crucial role in distinguishing signal from background and in positively identifying the 50% charm component in $L \to \nu q\bar{q}'$ decays.

ACKNOWLEDGMENTS

We thank K. Hikasa for discussion about the $Z \to \nu\bar{\nu}$ background. This research was supported in part by the University of Wisconsin Research Committee with funds granted by the Wisconsin Alumni Research Foundation, and in part by the U.S. Department of Energy under Contract No. DE-AC02-76ER00881.

[1]V. Barger *et al.*, Phys. Lett. **133B**, 449 (1983); Phys. Rev. D **29**, 2020 (1984).

[2]D. Cline and C. Rubbia, Phys. Lett. **127B**, 277 (1983); S. Gottlieb and T. Weiler, Phys. Rev. D **29**, 2005 (1984).

[3]V. Barger *et al.*, Nuovo Cimento **46A**, 622 (1978); V. Barger, J. Ohnemus, and R. J. N. Phillips, following paper, Phys. Rev. D **35**, 166 (1987).

[4]V. Barger and R. J. N. Phillips (unpublished), reported by V. Barger, in *Proceedings of the Oregon Meeting,* Annual Meeting of the Division of Particle and Fields of the APS, Eugeney, Oregon, 1985, edited by Rudolph C. Hwa (World Scientific, Singapore, 1986); in Proceedings of the Tenth Hawaii Conference on Particle Physics, Honolulu, 1985 (to be published); F. E. Paige (private communication) has independently used a similar approximation to W production.

[5]V. Barger and R. J. N. Phillips, Phys. Rev. Lett. **55**, 2752 (1985).

[6]V. Barger, N. Deshpande, R. J. N. Phillips, and K. Whisnant, Phys. Rev. D **33**, 1912 (1986).

[7]G. C. Fox and R. L. Kelly, in *Proton-Antiproton Collider Physics,* Madison, Wisconsin, 1981, edited by V. Barger, D. Cline, and F. Halzen (AIP Conf. Proc. No. 85) (AIP, New York, 1982), p. 432.

[8]R. Odorico, Nucl. Phys. **B228**, 381 (1983).

[9]T. Sjöstrand, Phys. Lett. **157B**, 321 (1985).

[10]F. E. Paige and S. D. Protopopescu, Report No. BNL-37066 1985 (unpublished).

[11]T. Gottschalk, Report No. Calt-68-1241, 1985 (unpublished).

[12]V. Barger, T. Gottschalk, J. Ohnemus, and R. J. N. Phillips, Phys. Rev. D **32**, 2950 (1985).

[13]V. Barger and R. J. N. Phillips, Phys. Lett. **122B**, 83 (1983).
[14]M. Glück, E. Hoffmann, and E. Reya, Z. Phys. C **13**, 119 (1982).
[15]D. W. Duke and J. F. Owens, Phys. Rev. D **30**, 49 (1984); E. Eichten, I. Hinchliffe, K. Lane, and C. Quigg, Rev. Mod. Phys. **56**, 579 (1984).
[16]K. Hikasa, University of Wisconsin Report No. MAD/PH/261 (unpublished); J. Cudell, F. Halzen, and K. Hikasa, Phys. Lett. **157B**, 447 (1985); G. Altarelli, R. Ellis, M. Greco, and G. Martinelli, Nucl. Phys. **B246**, 12 (1984); S. Ellis, R. Kleiss, and W. Stirling, Phys. Lett. **158B**, 341 (1985); **154B**, 435 (1985); S. Geer and W. Stirling, *ibid.* **152B**, 373 (1985).
[17]See, e.g., S. Komamiya, Heidelberg University Report No. HD-PY-86/01, 1986 (unpublished); in *Proceedings of the Twelfth International Symposium on Lepton and Photon Interactions at High Energies,* Kyoto, Japan, 1985, edited by M. Konuma and K. Takahashi (Research Institute for Fundamental Physics, Kyoto University, Kyoto, 1986).
[18]C. Peterson, D. Schlatter, I. Schmitt, and P. M. Zerwas, Phys. Rev. D **27**, 105 (1983).
[19]G. Arnison *et al.*, Phys. Lett. **147B**, 493 (1984).
[20]C. Rubbia, in *Proceedings of the Twelfth International Symposium on Lepton and Photon Interactions at High Energies,* Kyoto, Japan, 1985, edited by M. Konuma and K. Takahashi (Research Institute for Fundamental Physics, Kyoto University, Kyoto, 1986).
[21]V. Barger and R. J. N. Phillips, Nucl. Phys. **B250**, 741 (1985).